POWDERS & GRAINS 2017

Laboratoire Sols Solides Structures Risques

Communauté UNIVERSITÉ Grenoble Alpes

From continuum analytical description to discrete numerical modeling of localized fluidization in granular media

E.P. *Montellà*[1], M. *Toraldo*[1], B. *Chareyre*[1] and L. *Sibille*[1]

[1]Grenoble Institut of Technology (G-INP), University Grenoble Alpes (UGA), 3SR, F-38000 Grenoble, France

Introduction

Fluidization refers to the fluid-solids systems in which the solid phase in a granular material is subjected to behave like a fluid by an upward seepage flow.

A specific case concerns very localized influx of fluid, this situation is known as **localized fluidization**.

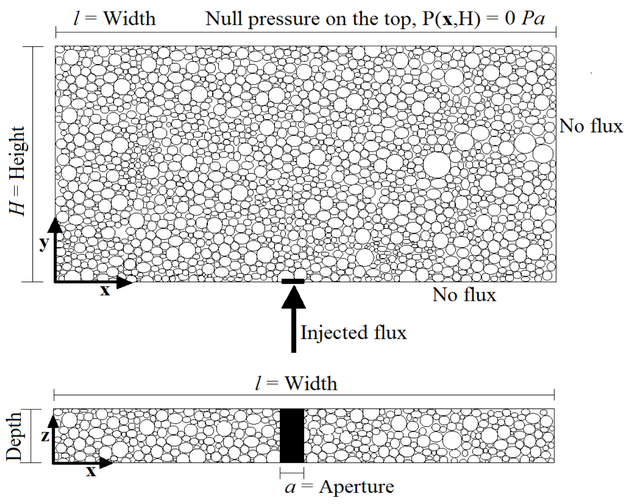

Figure 1. Sample geometry and boundary conditions. The granular layer is initially at static equilibrium then subjected to one or several local injections of fluid through the bottom face.

Previous works [1-3] on such configurations evidenced three successive regimes during a gradual increase of the injection rate:

- **Expansion regime**: Low rates cause bed expansion.

- **Cavity regime**: When flow rate increases, hydrodynamic forces counterbalance their weight, triggering fluidization above the injection point.

- **Chimney regime**: the height of the fluidized zone increases with the injection rate, until it reaches the top of the granular layer.

In this work, we present analytical and numerical approches results on the localized fluidization cavity within a grain packing originated when an upward flux is injected through the injection area.

Methodology

Coupled DEM-fluid model:

Numerical model based on the **DEM-PFV coupling** [4], assuming an incompressible fluid in the Stokes (viscous) regime.

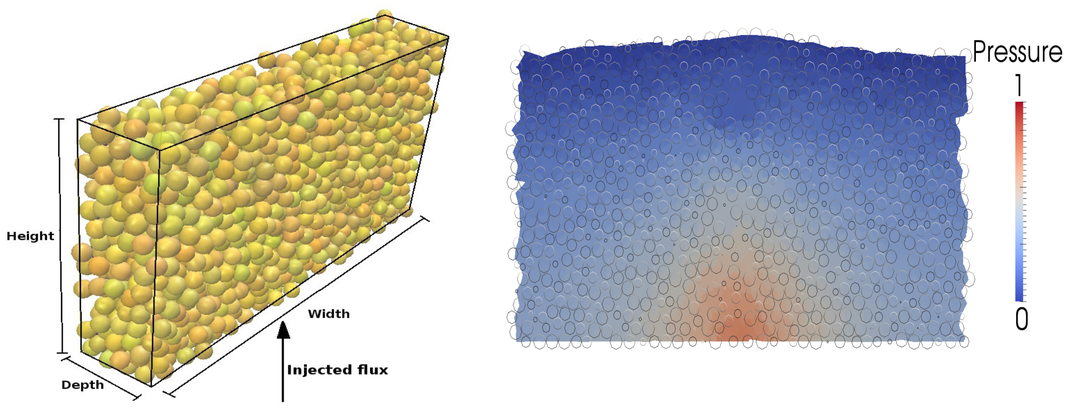

Figure 2. On the left, granular assembly geometry simulated by the numerical method. On the right, a 2D slice of the sample is displayed. Particles contour and dimensionless pressure field are shown. Fluidization begins when pressure balances the total stress (dimensionless pressure equal to 1).

Analytical solution:

The theoretical modeling determines the spatial distribution of pore pressure within the specimen identifying the locations in which it reaches (or exceeds) the total stress such that:

$$\sigma'^* := \frac{y-H}{H} + p^*(x,y) \geq 0, \qquad \text{where} \qquad p^* = \frac{P+\gamma_w(y-H)}{\sigma'_0}$$

is the normalized fluid pressure, σ'_0 is the vertical effective stress and P the fluid pressure.

Assuming Darcy's flow in a rigid porous layer (*figure 1*), following [5], the pressure at any point of the specimen can be obtained as:

$$P+\gamma_w y = \frac{q}{2\pi K}\int_{-a/2}^{a/2}\sum_{j=-\infty}^{\infty}\sum_{i=-\infty}^{\infty} -1^{|j|}\left[ln(\sqrt{(x-i\,l-s)^2+(y-j2H)^2})\right]ds$$

where K is the hydraulic conductivity, a the length of the aperture and q is the influx rate at the injection point.

Results and discussion

Single injection:

The different regimes described in the introduction can be distinguished in *figure 3* using the analytical solution. Low flux values correspond to the **expansion regime** in which no fluidization zone is detected (*figure 3a*).

As the flux increases, pore pressure keeps building up until it balances the total stress. Fluidized zone starts developing above the injection area, corresponding to the **cavity regime** (*figure 3b*).

Finally, the fluidized zone reaches the top of the sample, leading to a **chimney** of fluidized grains (*figure 3c*).

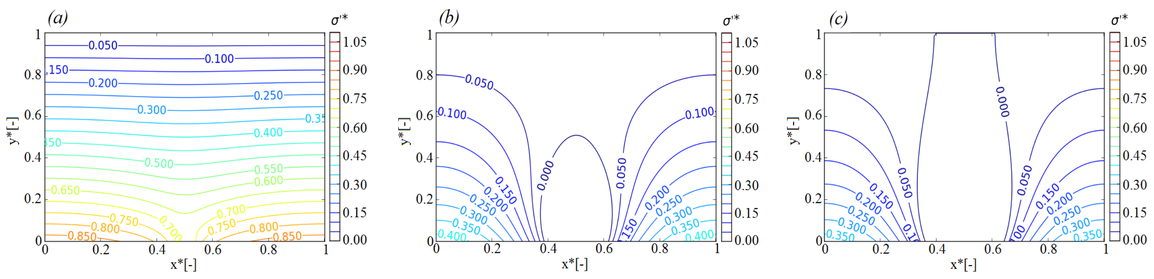

Figure 3. Evolution of the dimensionless effective stress σ' field when the injected flux increases using the theoretical solution.*

Main variables are presented in terms of dimensionless numbers. The relevance of the set of dimensionless variables is shown in *figure 4*. after running several numerical simulations with different parameters. A unique relationship between the normalized pressure p^* and normalized flux $q^* = \frac{q\mu}{D^2\sigma'_0}$ is found independent of the mean particle size D and fluid viscosity μ.

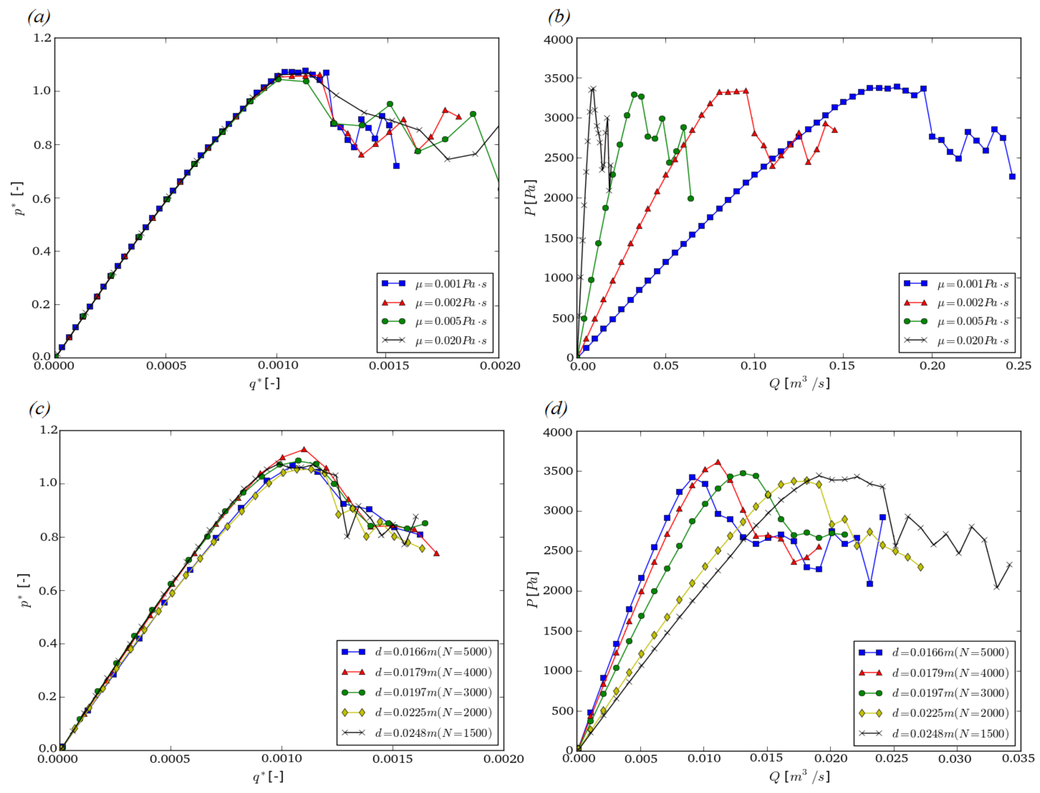

Figure 4. Sensitivity analysis on pressure-flux curves with injection aperture. Viscosity dependency with normalized p^*-q^* variables (a) and physical units (b); diameter dependency with normalized p^*-q^* variables (c) and physical units (d).

Regimes can be also observed by means of numerical simulation. *Figure 5* shows the evolution of porosity within the granular layer when the injected flux is increasing.

A "bubble" of high porosity is shown in *figure 5c*. This bubble is not fixed in time and space (the figure is only a snapshot at a given time) but tends to move up until it reaches the free surface.

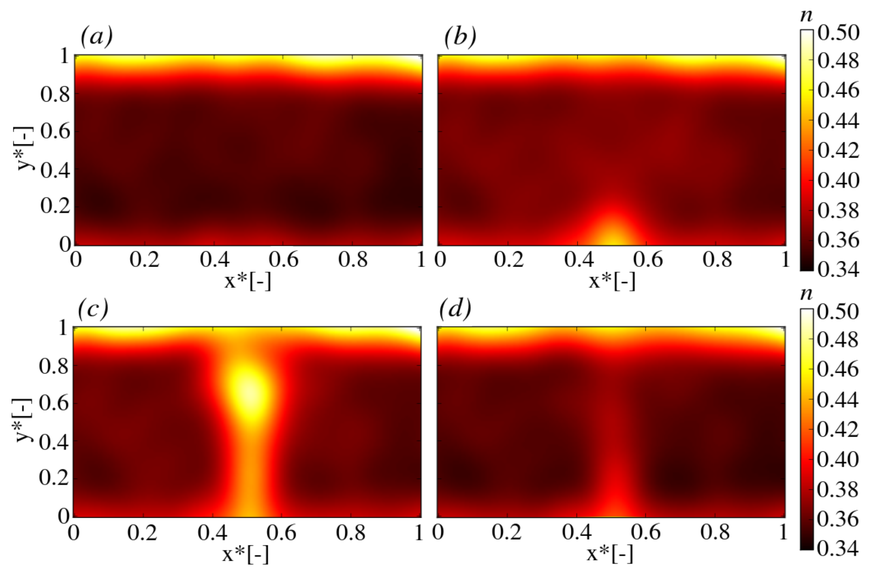

Figure 5. Evolution of the porosity for a narrow aperture. (a) Static regime. (b) Cavity regime. (c) Chimney regime. (d) injection rate is set back to zero. An irreversible increment of porosity (n≈ 0.42 locally) is observed above the injection point.

Two injections source:

Fluidized cavities developing above the injection points are strongly disturbed when two orifices of injection are close to each other. Based on the analytical approach, f*igure 6* evidences effective stress field at the time when the cavities resulting from two punctual sources are about two merge forming a single chimney.

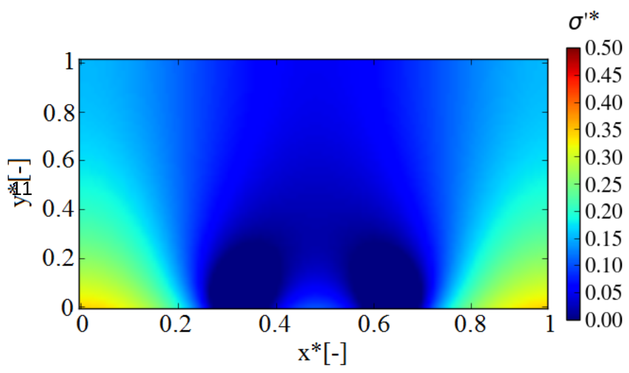

Figure 6. Dimensionless effective stress field for two punctual injections.

Bibliography

[1] Ngoma, J. and Philippe, P. and Bonelli, S. and Delenne, JY. and Radjai, F., *Geomechanics from Micro to Macro: Proc. of the Int. Symposium on Geomechanics from Micro to Macro, 4, 1571–1576, (2014)*

[2] Philippe, P. and Badiane, M. *Physical Review E 87, 042206, (2013)*

[3] Cui, X. and Li, J. Chan, A. and Chapman, D., *Powder Technology 254, 299-306, (2014)*

[4] Catalano, E. and Chareyre, B. and Barthélemy, E., *International Journal for Numerical and Analytical Method in Geomechanics 38, 51–71, (2014)*

[5] Montellà, E. P. and Toraldo, M. and Chareyre, B. and Sibille, L. *Physical Review E, 94(5), 052905, (2016)*